OPEN

Combination of secretin and fluvastatin ameliorates the polyuria associated with X-linked nephrogenic diabetes insipidus in mice

Giuseppe Procino[1,2,4], Serena Milano[1,4], Monica Carmosino[1], Claudia Barbieri[1], Maria C. Nicoletti[1], Jian H. Li[3], Jürgen Wess[3] and Maria Svelto[1,2]

[1]*Department of Biosciences, Biotechnologies and Biopharmaceutics, University of Bari, Bari, Italy;* [2]*Centro di Eccellenza di Genomica in Campo Biomedico ed Agrario (CEGBA), Bari, Italy and* [3]*National Institute of Diabetes and Digestive and Kidney Diseases, NIH, Bethesda, Maryland, USA*

X-linked nephrogenic diabetes insipidus (X-NDI) is a disease caused by inactivating mutations of the vasopressin (AVP) type 2 receptor (*V2R*) gene. Loss of V2R function prevents plasma membrane expression of the AQP2 water channel in the kidney collecting duct cells and impairs the kidney concentration ability. In an attempt to develop strategies to bypass V2R signaling in X-NDI, we evaluated the effects of secretin and fluvastatin, either alone or in combination, on kidney function in a mouse model of X-NDI. The secretin receptor was found to be functionally expressed in the kidney collecting duct cells. Based on this, X-NDI mice were infused with secretin for 14 days but urinary parameters were not altered by the infusion. Interestingly, secretin significantly increased AQP2 levels in the collecting duct but the protein primarily accumulated in the cytosol. Since we previously reported that fluvastatin treatment increased AQP2 plasma membrane expression in wild-type mice, secretin-infused X-NDI mice received a single injection of fluvastatin. Interestingly, urine production by X-NDI mice treated with secretin plus fluvastatin was reduced by nearly 90% and the urine osmolality was doubled. Immunostaining showed that secretin increased intracellular stores of AQP2 and the addition of fluvastatin promoted AQP2 trafficking to the plasma membrane. Taken together, these findings open new perspectives for the pharmacological treatment of X-NDI.

Kidney International advance online publication, 12 February 2014; doi:10.1038/ki.2014.10

KEYWORDS: cell and transport physiology; collecting ducts; diabetes insipidus; statins; vasopressin; water channels

Correspondence: *Giuseppe Procino, Department of Biosciences, Biotechnologies and Biopharmaceutics, University of Bari, Via Orabona 4, Bari 70126, Italy. E-mail: giuseppe.procino@uniba.it*

[4]These authors contributed equally to this work.

Received 30 April 2013; revised 6 December 2013; accepted 19 December 2013

The most recurrent genetic defects associated with hereditary nephrogenic diabetes insipidus (NDI) are the inactivating mutations of the vasopressin (AVP) receptor type 2 (*V2R*) gene that are localized on the X chromosome.[1–3] AVP binding to the V2R stimulates the trafficking of the aquaporin 2 (AQP2) water channel to the apical membrane of the collecting duct (CD) principal cells and also promotes AQP2 transcription.[4–10] Upon release into the systemic circulation, AVP (V2R) activates adenylyl cyclase, increases intracellular cyclic adenosine monophosphate (cAMP) levels, activates protein kinase A and other kinases, and phosphorylates AQP2. These events cause both the translocation of AQP2 storage vesicles to the apical plasma membrane and slow down AQP2 endocytic retrieval,[11] thus promoting water reabsorption in the CD.[6] In addition, V2R activation promotes phosphorylation of the cAMP-responsive element-binding protein and the expression of c-Fos. Binding of these factors to CRE and AP1 sites leads to AQP2 promoter activation.[12] Owing to the lack of functional V2Rs, AQP2 does not traffic to the plasma membrane and is substantially downregulated in X-linked NDI (X-NDI) patients and X-NDI mice.[13–16] As a consequence of the lack of AQP2 regulation, water reabsorption in the CD is severely impaired resulting in the production of large volumes (>30 ml/kg/day) of dilute urine (<250 mOsm/kg) (polyuria) and compensatory polydipsia. The main clinical characteristics of NDI include hypernatremia, hyperthermia, mental retardation, an overall failure to thrive, and repeated episodes of dehydration in early infancy.[1] So far, a targeted curative pharmacological therapy has not been developed for the treatment of X-NDI. The current first-line drug combination consists of hydrochlorothiazide (2–4 mg/kg per 24 h) and amiloride (0.3 mg/kg per 24 h).[17,18]

Many strategies have been proposed to bypass the defective V2R signaling and restore physiological AQP2 expression and/or trafficking.[15,19–28] In the last years, our group developed the first viable animal model of X-NDI.[15] We also showed that an prostaglandin E receptor subtype EP4 receptor agonist had a beneficial effect in X-NDI mice[15] and

that fluvastatin (FLU) induced AQP2 plasma membrane expression *in vivo*, independent of V2R stimulation.[24]

Several studies suggest that hormones other than AVP, such as secretin (SCT), also exhibit antidiuretic functions.[29] The SCT receptor (SCTR) is a G protein-coupled receptor (GPCR) known to couple to both Gs and Gq, with the stimulatory cAMP response being most prominent and sensitive.[30]

Of note, SCTR-null mice display mild polyuria, polydipsia, distension of the renal pelvis, and reduced renal expression of AQP2.[31] The same authors showed that SCTR is expressed in the kidney medulla,[31] in agreement with previously published data.[32] However, a clear demonstration of a direct action of SCT on AQP2 transcription and trafficking is still missing.

Here we demonstrate that the SCTR is expressed at the basolateral membrane of AQP2-expressing CD principal cells, prompting us to analyze the effect of SCT *ex vivo* on kidney slices and *in vivo* in *V2R-KO* mice[15] (X-NDI mice).

We provide compelling evidence that SCT increases cAMP concentrations in CD tubule suspensions and promotes AQP2 apical expression in kidney slices. In X-NDI mice, chronic infusion with SCT increases AQP2 abundance but not its apical expression. Of note, in SCT-infused X-NDI mice, a single injection of FLU, a drug that induces AQP2 membrane accumulation in wt C57BL/6 mice,[24] promotes AQP2 membrane expression and greatly improves the urine concentration ability.

RESULTS

SCTR expression in mouse and human kidney

We first used reverse transcriptase-PCR (RT-PCR) to evaluate the presence of SCTR transcripts in different regions of the mouse kidney. SCTR expression was clearly detectable in total RNA samples extracted from mouse inner medulla (IM), outer medulla (OM), and cortex (CTX; Figure 1a). Sequencing confirmed the specificity of the obtained bands (data not shown).

We next examined SCTR protein expression in mouse kidney by western blotting. Total protein extracts from IM, OM, and CTX were analyzed, along with protein extracts from mouse brain, cerebellum, liver, heart, and pancreas, all tissues expressing SCTR. A protein band of the expected molecular mass (52 kDa) was immunodetected in all samples. SCTR expression was more abundant in the kidney OM and CTX compared with the IM (Figure 1b). The specificity of the band obtained with the anti-SCT affinity-purified antibody (Ab) was tested by pre-adsorbing the Ab with the immunizing peptide (Figure 1b).

Unfortunately, we could not perform SCTR immunolocalization studies in mice as the SCTR Ab, which was raised against a synthetic peptide corresponding to the human SCTR sequence, proved unsuitable for immunofluorescence studies in mouse kidney. On the other hand, we carried out SCTR immunolocalization studies in human kidney sections from kidney CTX using the same Ab. Sections were stained

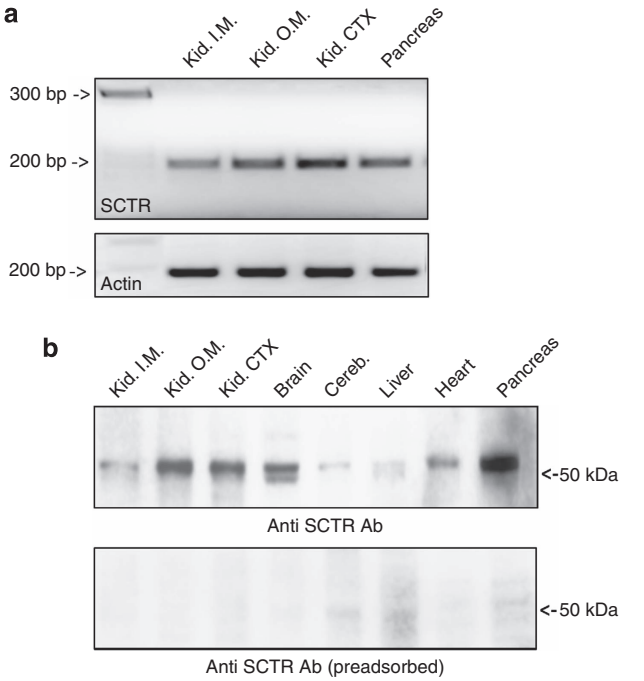

Figure 1 | Analysis of the expression of secretin receptor (SCTR) in the mouse kidney by reverse transcriptase-PCR (RT-PCR) and western blotting. (**a**) Total RNAs extracted from kidney inner medulla (IM), outer medulla (OM), cortex (CTX), and pancreas were probed for the presence of mRNA encoding SCTR. Specific bands were obtained in all kidney fractions. Control RT-PCR was performed using primers amplifying mouse beta-actin mRNA. Three independent experiments were carried out. (**b**) Total protein extract from mouse kidney IM, OM, and CTX, were separated by sodium dodecyl sulfate-polyacrylamide gel electrophoresis (SDS-PAGE) and immunoblotted for the presence of SCTR. Mouse brain, cerebellum, liver, heart, and pancreas were used as additional controls. The specificity of the immunodetected band was demonstrated using anti-SCTR antibodies pre-adsorbed on the immunizing peptide. Three independent experiments were carried out.

with the anti-SCTR Ab and co-stained with anti-AQP2, AQP3, and Na^+/K^+-ATPase Abs, after which images were obtained with laser confocal-scanning microscopy. Figure 2a shows that SCTR fluorescence specifically decorated the basolateral membrane of AQP2-positive cells. In particular, we colocalized SCTR with two basolateral markers: AQP3 and Na^+/K^+-ATPase. Confocal analysis indicated a significant degree of colocalization of SCTR with both basolateral membrane markers (Figure 2a and b, overlay, ×3 magnification insets).

SCTR staining was also detected in other kidney tubules that were not stained by the anti-AQP2 Ab. We were also able to identify SCTR staining in the Tamm–Horsfall-positive tubule, thus strongly indicating that, besides the CD system, SCTR is also expressed in the thick ascending limb of Henle's loop within the kidney (Figure 2c). Of note, being both anti-SCTR and anti-THP Abs produced in rabbit, we used two sequential human kidney sections.

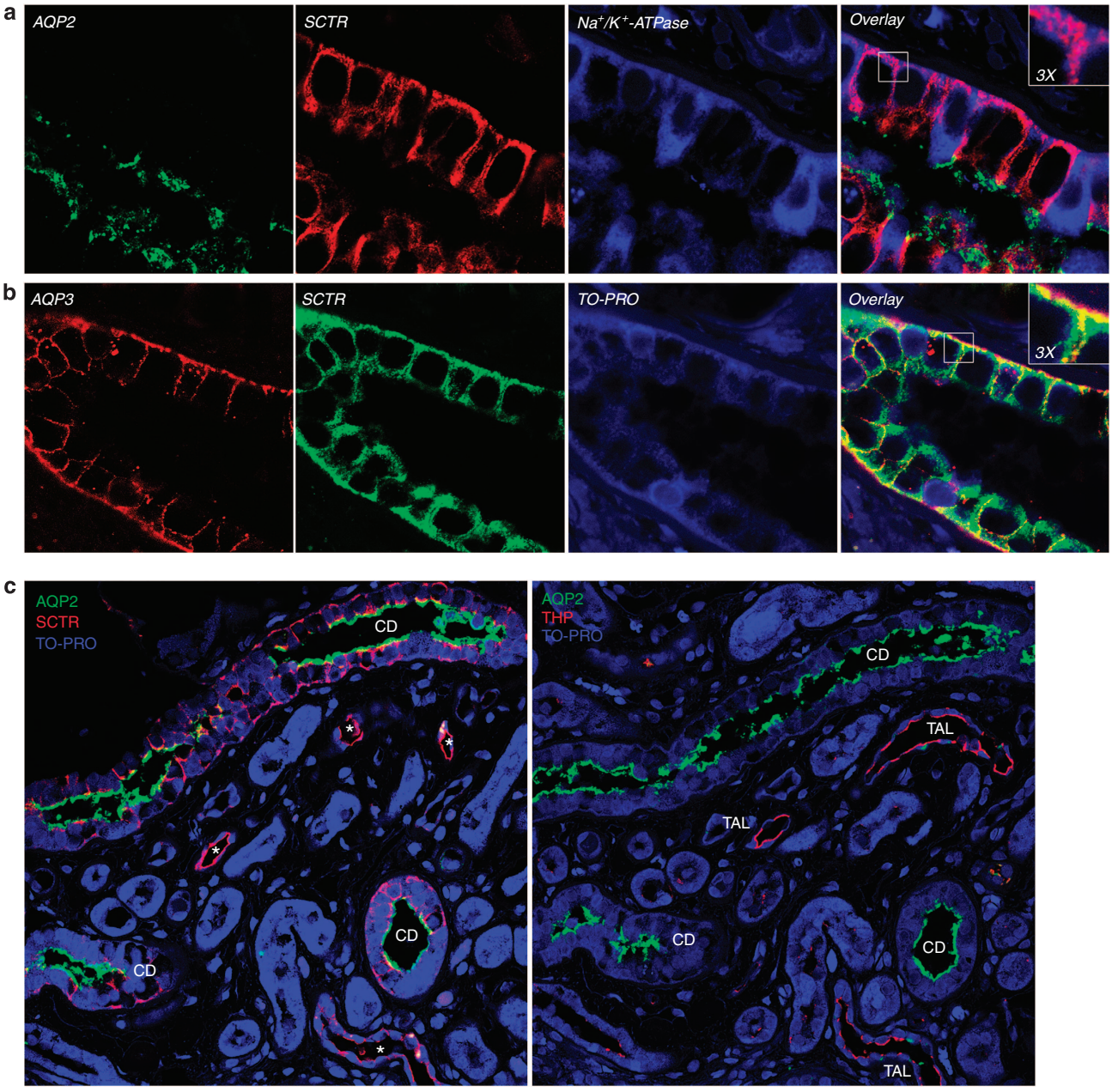

Figure 2 | Immunolocalization of secretin receptor (SCTR) in human kidney sections. Immunofluorescence detection of SCTR in human kidney. (**a**) SCTR was stained with Alexa Fluor-555 (red), aquaporin 2 (AQP2) was stained with Alexa Fluor-488 (green), and Na^+/K^+-ATPase with Alexa Fluor-633 (blue). AQP2 was seen at the apical pole of the collecting duct (CD) principal cells, whereas the SCTR antibody decorated the basolateral membrane of the same cells and colocalized with the basolateral marker Na^+/K^+-ATPase (pink color in the ×3 magnified signal). (**b**) SCTR was stained with Alexa Fluor-488 (green), AQP3 was stained with Alexa Fluor-555 (red), tissue counterstained with TO-PRO (blue). SCTR largely colocalized with AQP3 at the basolateral membrane of CD cells (yellow color in the ×3 magnified signal). (**c**) Co-immunostaining in serial sections using AQP2 (green) as marker of the CD and Tamm–Horsfall protein (THP, red) as marker of the thick ascending limb (TAL). SCTR-positive tubules (asterisks) were also positive for THP. Magnification ×60.

SCTR is functionally expressed in mouse kidney and regulates AQP2 exocytosis via cAMP increase

We next incubated freshly isolated mouse inner medullary CD (IMCD) suspensions with either 1-deamino-8-D-arginine-vasopressin (dDAVP) or SCT and measured changes in intracellular cAMP concentrations. Treatment with either SCT or dDAVP led to concentration-dependent increases in intracellular cAMP levels in wt mice (Figure 3a, wt mice). The magnitude of the dDAVP-mediated cAMP response was greater than that of the corresponding SCT response. In addition, SCT was also able to increase cAMP concentration in IMCD suspension isolated from X-NDI mice (Figure 3a, X-NDI mice).

Next, we stimulated SCTR with its physiological ligand SCT in mouse kidney slices *in vitro*. Interestingly, 10^{-7} mol/l

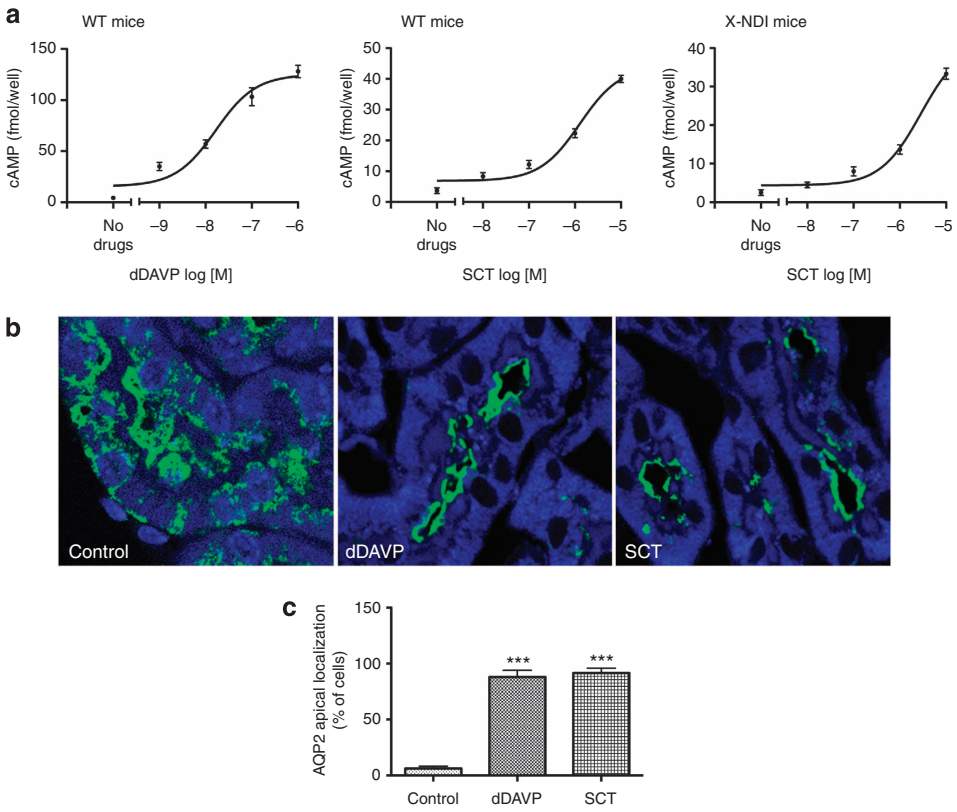

Figure 3 | Effect of treatment with secretin (SCT) and dDAVP on cyclic adenosine monophosphate (cAMP) concentrations and AQP2 plasma membrane localization on kidney collecting ducts. (**a**) SCT and dDAVP-induced cAMP production in mouse inner medullary collecting duct (IMCD) tubule suspensions. Freshly isolated IMCD tubule suspensions from C57BL/6 WT or tamoxifen (TMX)-induced X-linked nephrogenic diabetes insipidus (X-NDI) mice (12-week-old males; $n = 8$ per individual experiment) were pooled and equally distributed into 24-well plates. Samples were treated with the indicated concentrations of dDAVP or SCT for 60 min at 37 °C. Total cAMP generated in each well was normalized to the amount of protein present in each well. Three independent experiments were carried out. Data are provided as mean ± s.e.m. (**b**) Indirect immunofluorescence images of kidney tissue slices showing AQP2 in principal cells of collecting ducts (CDs). One C57BL/6 WT mouse kidney was cut into thin slices and incubated *in vitro* with buffer alone (control) or with dDAVP 10^{-7} mol/l or SCT 10^{-7} mol/l for 1 h before fixation by immersion, sectioning, and immunostaining to detect AQP2. Under control conditions, AQP2 was mainly localized throughout the cytoplasm and showed little apical membrane staining in CDs. In the presence of dDAVP or SCT, AQP2 staining of the apical membrane region was increased in principal cells of the cortical CD. The images are representative of three independent experiments. (**c**) Quantification of the number of cells displaying plasma membrane (PM) localization was determined by counting the fraction of cells showing apical PM localization. The extent of translocation is expressed as the percentage (means ± s.e.) of cells showing a continuous apical PM localization in at least 100 randomly chosen CD principal cells from three independent determinations. Quantitation of cells displaying AQP2 apical membrane expression expressed as a percentage of total cells observed. ***$P < 0.0005$ with Student's *t*-test. dDAVP, 1-deamino-8-D-arginine-vasopressin.

of SCT was as effective as 10^{-7} mol/l of dDAVP in promoting AQP2 trafficking toward the luminal plasma membrane when compared with the cytoplasmic localization of AQP2 observed in control slices (Figure 3b). Quantification of the relative extent of dDAVP- and SCT-stimulated AQP2 translocation is shown in Figure 3c. Plasma membrane translocation was determined by visualization on a Leica SP2 confocal microscope analyzing >100 randomly chosen CD principal cells per condition. The number of cells displaying a complete redistribution of the staining toward the apical plasma membrane was calculated as a percentage of all counted cells and expressed as means ± s.e. from three independent experiments.

We observed clear AQP2 apical accumulation in about 90% of the cells observed both in the CTX and in the medulla.

Characterization of NDI phenotype of V2R$^{fl/y}$Esr1-Cre mice and effect of SCT infusion on urinary parameters

We previously described the first viable mouse model of X-NDI.[15] In these mutant mice, the *V2R* gene can be deleted in a conditional (tamoxifen (TMX)-dependent) manner in the kidneys of adult mice. The resulting V2R-KO mice (X-NDI mice) show all key symptoms of X-NDI, including the production of large amounts of dilute urine (polyuria) and polydipsia.[15] Eight-week-old V2R$^{fl/y}$Esr1-Cre mice (littermates) were placed into metabolic cages, and 24-h urine volume and osmolality, along with water intake and body weight, were measured daily for a period of 13 days. The resulting data are reported in Supplementary Figure 1 online. After 2 days of acclimatization to the new environment (days –2, –1), on day 0 half of the mice received a single daily intraperitoneal (i.p.) injection of 4-hydroxytamoxifen

(4-OH)-TAX (0.5 mg per mouse) for the following 6 days. As reported previously,[15] TMX treatment triggered marked increases in diuresis and water intake, accompanied by a pronounced reduction in urine osmolality (Supplementary Figure 1 online). We did not observe significant changes in the severity of the NDI phenotype up to 6 months after TMX treatment (data not shown).

A detailed western blotting analysis of AVP-regulated renal aquaporins (AQP2, 3) expressed in the kidney CTX, OM, and IM is reported in Supplementary Figure 2 online. This analysis was performed on $V2R^{fl/y}$Esr1-Cre mice 20 and 60 days after the suspension of TMX treatment and the western blot data were compared with those of non-induced animals. Strikingly, in the TMX-treated mice, we observed a marked downregulation of AQP2 and AQP3 in all kidney portions that were investigated (Supplementary Figure 2 online), in line with previously reported data.[15]

Given the *in vitro* effects of SCT on AQP2 trafficking as described above, we next examined whether infusion of X-NDI mice with SCT was able to promote AQP2 expression and plasma membrane translocation. For these experiments, we used $V2R^{fl/y}$Esr1-Cre mice 5 months after TMX induction. Unfortunately, a single injection of SCT at physiological doses (nanomolar) failed to produce any effect on mice diuresis or urine osmolality (data not shown). Given the short half-life of SCT[33] and the marked downregulation of AQP2 in X-NDI mice, we opted for a continuous infusion for longer times. Six mice were subcutaneously implanted with osmotic minipumps (Alzet) loaded with a SCT solution and continuously infused for 14 days at a SCT dose of 1 nmol/kg/day at constant rate (+SCT). Control animals ($n=6$, littermates) received minipumps loaded with saline alone (−SCT). Diuresis, urine osmolality, and water intake were recorded daily for the entire duration of the treatment. Diuresis and urine osmolality did not significantly change in SCT-treated animals (Figure 4a). At the end of the studies, the animals were killed and kidneys were used for real-time RT-PCR, western blotting, and immunofluorescence analysis reported in Figure 4b, c, and d, respectively.

Total kidney homogenates from TMX-induced $V2R^{fl/y}$ Esr1-Cre mice (X-NDI mice), treated or not with SCT, and $V2R^{fl/y}$Esr1-Cre littermates that had not received TMX (control, CTR) were used for quantitative RT-PCR and immunoblotting with anti-AQP2 Ab. Real-time RT-PCR indicated that SCT infusion alone doubled AQP2 gene transcription levels compared with those in saline-infused animals (Figure 4b). In Figure 4c, a lysate of wt mice IM (ms. IM) was loaded in the first lane as positive control for AQP2 immunodetection. The strong signal detected in this fraction, compared with all the whole-kidney preparations, is due to the high abundance of AQP2 in the IM of wt mice. Interestingly, semiquantitative analysis showed that AQP2 abundance was increased by 90% in SCT-infused animals (+SCT) compared with saline-infused animals (−SCT, Figure 4c). AQP3 expression was unchanged after SCT infusion (data not shown).

Immunofluorescence analysis of contralateral kidney sections supported the results obtained by western blotting: the number of AQP2-positive tubules was clearly increased and AQP2 fluorescent signal was clearly brighter as compared with that of saline-infused animals (Figure 4c). However, at a higher magnification (Figure 4c, magnified), AQP2 was mainly localized within the cell cytoplasm with negligible expression at the apical plasma membrane.

Association of SCT and FLU improves urinary parameters in X-NDI mice

We previously reported that the treatment of wt mice with FLU induced a transient accumulation of AQP2 at the apical membrane of the CD principal cells and increased water reabsorption in an AVP-independent manner.[24] We therefore examined the ability of FLU to promote AQP2 membrane localization in SCT-infused $V2R^{fl/y}$ Esr1-Cre mice. Mice were treated as above with SCT-loaded osmotic minipumps, except that half of both the SCT and control groups received a single i.p. injection of FLU (50 mg/kg) on the last day of SCT treatment. The other half of animals was injected with the same volume of saline solution. We measured cumulative urine output and urine osmolality for 6 h following FLU injection (Figure 5).

Strikingly, urine production of SCT-infused animals that had received FLU was reduced by nearly 90% as compared with both untreated and SCT-treated animals (Figure 5, SCT + FLU). SCT alone had no effect on diuresis, in agreement with experiments shown in Figure 4a, whereas FLU alone had a small but significant effect. Moreover, urine osmolality was significantly increased (~2-fold) in the SCT-infused mice that had received FLU. Blood was taken for sinistrin-fluorescein isothiocyanate clearance determinations (see Materials and Methods section) and estimation of glomerular filtration rate (GFR). GFR of SCT + FLU-infused mice was 317.3 ± 14.89 µl/min, which was statistically higher than that of saline-infused animals (218.3 ± 9.28 µl/min) as reported in Table 1.

At the end of the treatment, X-NDI mice were killed and the immunolocalization of renal AQP2 was examined by immunofluorescence (Figure 6). Non-induced animals were analyzed in parallel (top panels).

The most striking difference between non-induced (−TMX) and TMX-induced (+TMX) X-NDI mice was the abundance of AQP2 in all kidney portions examined. In fact, in TMX+ X-NDI mice, AQP2-positive CDs were rare and poorly immunoreactive to AQP2 Abs compared with TMX− animals (Figure 6, CTR). In FLU-injected X-NDI mice, the low residual AQP2 was localized to the apical plasma membrane (Figure 6, Flu). SCT infusion for 14 days clearly increased the number and the immunoreactivity to AQP2 Ab of CDs (Figure 6, SCT). However, observation of kidney CDs at higher magnification clearly indicated that AQP2 was

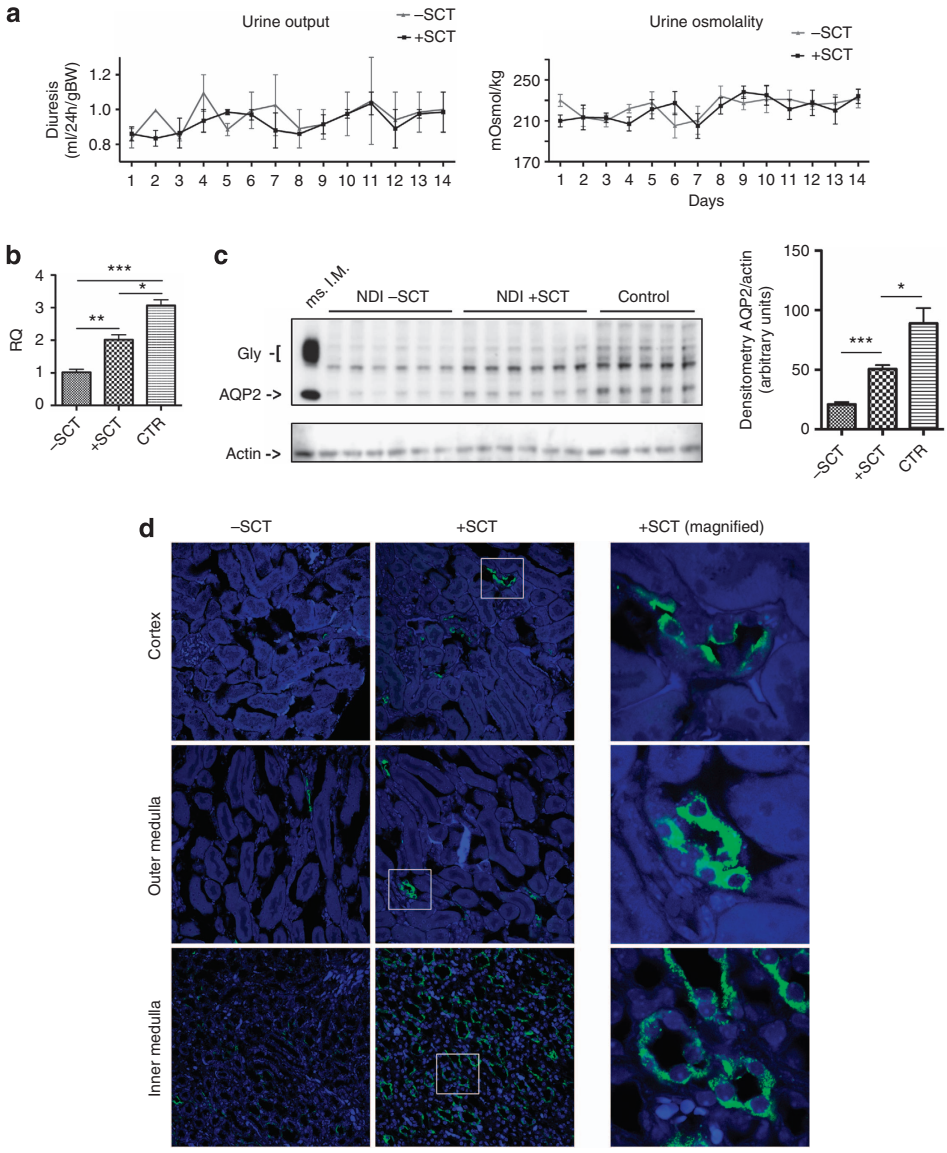

Figure 4 | Effect of prolonged infusion of X-linked nephrogenic diabetes insipidus (X-NDI) mice with secretin (SCT) on urine output, urine osmolality, aquaporin 2 (AQP2) abundance, and membrane expression. (**a**) Five months after the end of the tamoxifen (TMX)-injection period, X-NDI mice were subcutaneously implanted with osmotic minipumps and continuously infused with saline alone or SCT at a dose of 1 nmol/kg/day over a 14-day period. Urine output, normalized for body weight, and osmolality were measured daily. No significant changes in urinary parameters were seen in SCT-infused animals. (**b**) At the end of the experiment, quantitative reverse transcription polymerase chain reaction was performed on kidneys from X-NDI infused with saline (− SCT) or with secretin (+ SCT). Control animals that did not receive TMX were included (CTR). Relative quantification of gene expression (RQ) was performed setting the amount of AQP2 mRNA in vehicle-infused animals (− SCT) as 1. SCT-infused animals exhibited an approximately twofold increase in *AQP2* gene transcription compared with saline-infused mice. (*$P<0.05$, **$P<0.005$, ***$P<0.0005$ with Student's *t*-test, $n=6$ per group.) (**c**) Western blotting with anti-AQP2 antibodies was carried out using homogenates prepared from whole left kidneys. Kidneys from control animals of the same age that had not received TMX were used as control. Protein extract from mouse inner medulla (IM) was loaded as positive control for AQP2 immunodetection. 29 kDa AQP2 band (AQP2) and glycosylated AQP2 band (gly) are indicated. Densitometric analysis of AQP2 bands, normalized for the actin abundance in each fraction, is reported on the right indicating that SCT infusion promoted a nearly 90% increase of AQP2 abundance. (**d**) The right kidneys were subjected to immunofluorescence localization of AQP2 in the three kidney regions. The number of AQP2-positive CD cells and the intensity of AQP2 fluorescence were increased in SCT-infused animals. Observation of single tubules at higher magnification (right panels) unambiguously showed that AQP2 was localized intracellularly. The experiment was repeated three times and comparable results were obtained. *$P<0.05$; ***$P<0.0001$; $N=6$ per group.

localized mainly intracellularly (Figure 6, SCT, inset). Remarkably, after FLU treatment in SCT-infused mice, AQP2 was predominantly expressed at the apical plasma membrane (Figure 6, SCT + Flu).

DISCUSSION

In this study, we provide strong evidence that combined administration of SCT and FLU increases AQP2 plasma membrane expression in X-NDI mice and improves the

Table 1 | FE of Na^+ and K^+ and GFR measured in control X-NDI mice (CTR) and in animals after the combined treatment with SEC and FLU (SCT + FLU)

	CTR	SCT + FLU
FENa%	0.7933 ± 0.05812	0.2333 ± 0.03528**
FEK%	34.20 ± 1.562	17.60 ± 1.058***
GFR (μl/min)	218.3 ± 9.280	317.3 ± 14.89**

Abbreviations: FE, fractional excretion; FLU, fluvastatin; GFR, glomerular filtration rate; SCT, secretin; X-NDI, X-linked nephrogenic diabetes insipidus.
**$P < 0.05$; ***$P < 0.001$.

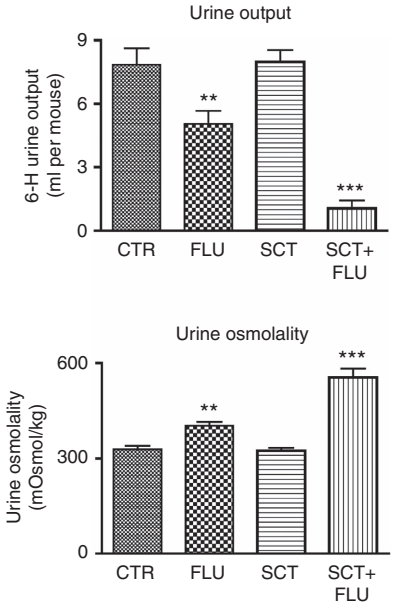

Figure 5 | Combination of prolonged secretin (SCT) infusion and a single fluvastatin (FLU) injection markedly ameliorates nephrogenic diabetes insipidus (NDI) symptoms in X-linked NDI (X-NDI) mice. Five months after the end of tamoxifen (TMX)-injection period, X-NDI mice were subcutaneously implanted with osmotic minipumps and continuously infused with either saline alone or SCT at a dose of 1 nmol/kg/day over a 14-day period. On the last day of SCT infusion, half of the control and SCT-infused mice were given an intraperitoneal (i.p.) injection of FLU (50 mg/kg) and urine output and osmolality were monitored for the following 6 h. Compared with untreated animals (CTR), FLU alone had a slight effect on urine output and urine osmolality. As already shown in Figure 4, SCT alone had no significant effect on urinary parameters. Interestingly, a single FLU injection in SCT-infused mice (SCT + FLU) led to a marked reduction of urine output, accompanied by a significant increase of urine osmolality. Data are presented as mean ± s.e.m. **$P < 0.05$; ***$P < 0.001$. $N = 5$ per group.

kidney concentration defect of these animals. X-NDI is characterized not only by the lack of plasma membrane trafficking of AQP2 but also by a severe downregulation of AQP2 protein expression. Both phenomena result from the inactivation of V2R signaling in the principal cells of the CDs. Consequently, strategies aimed at correcting the described AQP2 deficits may offer novel therapeutic opportunities for X-NDI therapy.

One possible approach to bypass V2R function in the CD principal cells is to activate other GPCRs coupled to Gs/adenylyl cyclase. We already showed that a compound that selectively activates the prostaglandin E receptor subtype EP4 is highly effective in ameliorating all major manifestations of X-NDI.[15] Here we investigated the presence and the activity of SCTR in the mouse and human CD and its possible role in regulating AQP2 expression and trafficking.

We previously reported a detailed analysis of the GPCRs expressed by IMCD cells.[15] Interestingly, several GPCRs expressed by IMCD cells (Gpr56, Gpr116, Gpr125, and Gpr97) belong to the SCT-like family-2 of GPCRs, although the endogenous ligands have not been identified for these receptors. Another piece of evidence, supporting the presence of SCTR in the CDs and its possible role in regulating AQP2, comes from the work of Chu *et al.*[31] who reported that $SCTR^{-/-}$ mice show reduced renal expression of AQP2, associated with mild polyuria and polydipsia. The possible involvement of SCT in regulating water reabsorption in the kidney via AQP2 membrane expression is also suggested by the observation that SCT plasma levels are increased during water deprivation in normal rats but not in hypophysectomized animals.[21]

In this study, we show by western blotting that the Gs-coupled SCTR is expressed in the mouse kidney in the CTX, OM, and IM. We also performed immunolocalization studies of SCTR in human kidney sections and clearly showed, for the first time, that SCTR is localized to the basolateral membrane of AQP2-expressing cells and in the thick ascending limb. The observation that SCTR is expressed in the kidney CDs is essential for attempts to target this receptor for therapeutic purposes in X-NDI patients lacking proper V2R function.

We also report that, *ex vivo*, short-term SCT stimulation of the SCTR induced a dose-dependent rise in intracellular cAMP concentrations in the CDs and in AQP2 translocation from intracellular vesicles to the plasma membrane in freshly isolated kidney slices from CTR and X-NDI mice.

To explore the potential usefulness of SCT for the therapy of X-NDI, we treated X-NDI mice with SCT. As the estimated half-life of circulating SCT is very short (1.5–5 min),[33] and single injection had no effect in our experimental model, we delivered SCT continuously in the systemic circulation using osmotic minipumps. Exogenous SCT was infused at the rate of 1 nmol/kg/day, comparable to rates previously reported by other authors,[34,35] and was able to increase the SCT plasma concentration above the physiological range.[35] The most striking effect of SCT infusion was the upregulation of AQP2 mRNA and protein expression in the kidneys of X-NDI mice. Unfortunately, the increased expression of AQP2 *per se* was insufficient to ameliorate the X-NDI phenotype, as AQP2 remained intracellular.

The effects evoked by short- and long-term stimulation of SCTR on AQP2 trafficking and expression may seem to be in apparent contradiction to each other. However, it is not surprising that stimulation of GPCR with a persistent ligand is followed by several distinct mechanisms of desensitization that attenuate receptor signaling.

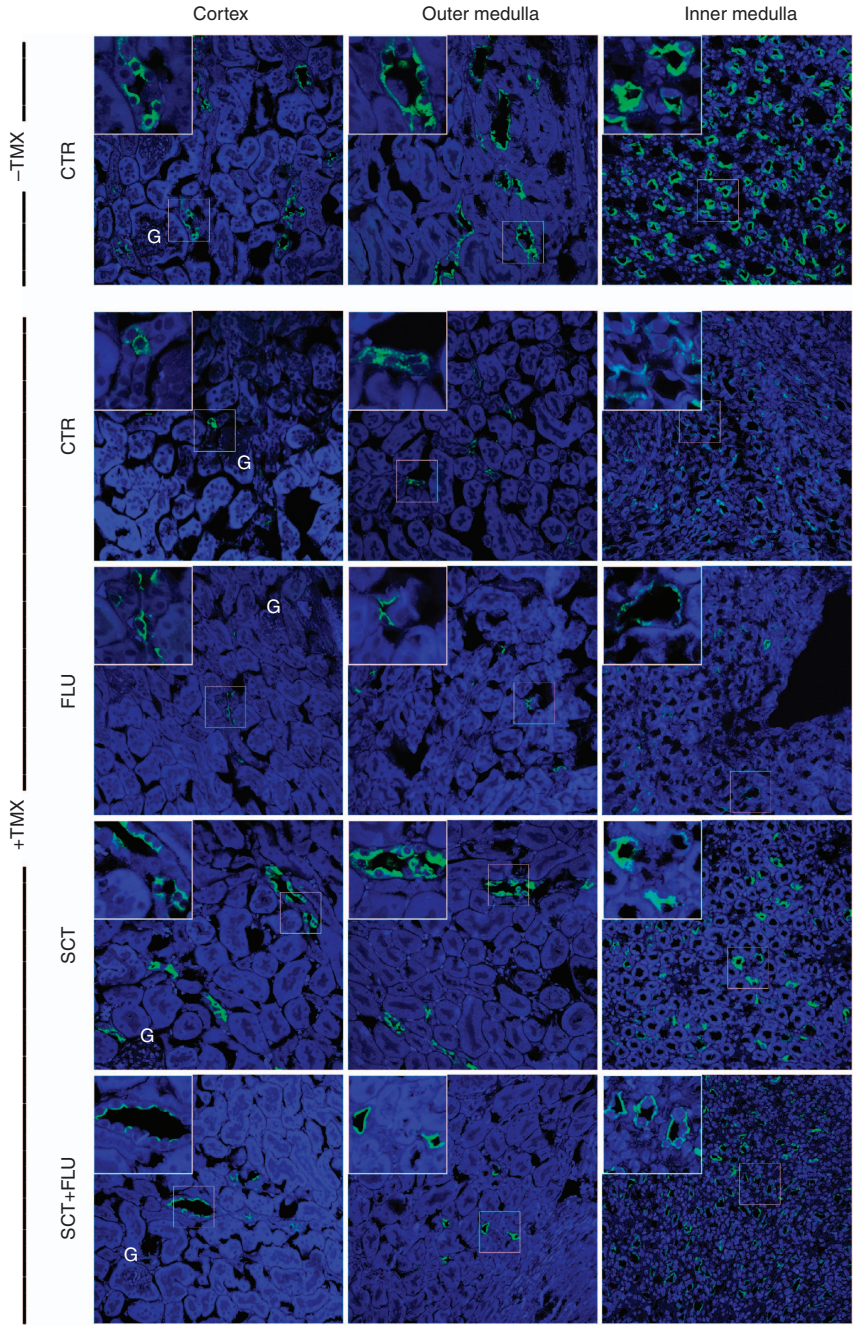

Figure 6 | Combination of prolonged secretin (SCT) infusion and a single fluvastatin injection upregulates aquaporin 2 (AQP2) expression and promotes AQP2 plasma membrane localization in X-linked nephrogenic diabetes insipidus (X-NDI) mice. At the end of the treatment described in Figure 5, mice were killed and their kidneys subjected to AQP2 immunolocalization followed by confocal examination. V2R$^{fl/y}$*Esr1-Cre* mice of the same age that had not received tamoxifen (−TMX) were analyzed in parallel. Random pictures were taken in the kidney cortex, outer medulla, and inner medulla. A high magnification of a detail of each image is shown in the upper left corner of each panel. Compared with non-induced animals (−TMX, CTR), mice with V2R deletion (+TMX, CTR) showed a marked reduction of AQP2 immunoreactivity in each kidney portion. FLU injection triggered the accumulation of the remaining amount of AQP2 on the luminal membrane. SCT infusion greatly upregulated AQP2 immunoreactivity in the kidney collecting ducts (CDs). At higher magnification, AQP2 was seen mainly in the cytoplasm with negligible plasma membrane expression. In mice chronically infused with SCT and injected with fluvastatin (SCT + FLU), AQP2 was upregulated and mainly expressed at the luminal membrane of CD tubules. Representative images are shown ($N = 5$). G, glomerulus.

At present, we do not have an explanation for the lack of AQP2 plasma membrane expression observed after prolonged (14 days) stimulation with SCT, but SCTR desensitization may have a role in this phenomenon. It has been demonstrated that SCTR undergoes a rapid desensitization within minutes after exposure to its ligands to prevent

cellular overstimulation.[36–38] We can hypothesize that the residual SCTR activity may be sufficient for boosting AQP2 transcription but too low to induce AQP2 membrane expression. Recent work with the mpkCCD mouse cell line has shown that the long-term regulation of AQP2 by AVP occurs independent of protein kinase A and cAMP-responsive element-binding protein, but may involve the exchange factor directly activated by cAMP (Epac).[39] In particular, these authors demonstrated that after 4 days of dDAVP stimulation, cAMP intracellular concentrations are lower than those measured after 30 min or 1 day of stimulation, although AQP2 levels were still sustained. On the basis of these observations, prolonged stimulation of SCTR in mouse kidney may result in similar long-term effects: cAMP responses may become partially blunted, leading to impairment in protein kinase A activation and AQP2 exocytosis. At the same time, Epac activation may be sufficient to sustain AQP2 transcription. Such a mechanism would explain our findings that AQP2 is upregulated but shows a preferential cytoplasmic localization in SCT-infused X-NDI mice.

We previously reported that FLU treatment leads to translocation of AQP2 *in vivo* in wt mice.[24] We show here that FLU treatment alone has a slight effect on the urine concentrating ability of X-NDI mice, most likely due to the very low levels of AQP2 expressed by these mutant mice. Strikingly, however, FLU treatment of SCT-infused X-NDI mice led to a marked reduction of the diuresis with no impairment of the GFR (Table 1).

The fact that in SCT + FLU-treated mice urine volume is reduced by 90%, whereas urine osmolality only doubles may also indicate that solute reabsorption is increased in kidney tubules by this combined treatment. An additional possible target of SCT action may be the thick ascending limb of Henle's loop and in particular the cotransporter NKCC2.[40] We showed here by immunofluorescence that SCTR is also expressed in the thick ascending limb. We also showed that in X-NDI mice, following the combination of SCT and FLU, the fractional excretion of Na^+ and K^+ was significantly reduced (Table 1), thus suggesting that increased solute reabsorption is promoted in these mice in which the cortico-medullary osmotic gradient is compromised in the absence of V2R signaling. Further investigation is needed to address this interesting aspect.

We recently showed the proof of principle that high doses of FLU can increase AQP2 plasma membrane expression in the kidney CDs of wt mice.[24] We also identified some of the intracellular targets of statins that could explain the effect on AQP2 membrane expression and hypothesized that reduced prenylation of RhoA and Rab5 may explain AQP2 membrane accumulation.[24] Consistent data were also obtained on Brattleboro rats infused with simvastatin.[22] These observations imply that different drugs, acting downstream of the cholesterol biosynthetic pathway step inhibited by statins, in particular inhibitors of geranylgeranyl transferases,[41] may be useful as regulators of AQP2 trafficking. Alternatively, the development of new classes of statins with prolonged half-life and preferential kidney delivery may allow the use of much lower doses of these agents for the treatment of X-NDI.

It should be noted that recombinant SCT is already approved for use in humans in the diagnosis of gastrointestinal disorders and FLU is Food and Drug Administration approved for clinical use since 1993.

In conclusion, we have shown that prolonged SCT infusion greatly rescues AQP2 protein downregulation in X-NDI mice. In addition, FLU treatment of SCT-infused X-NDI mice effectively promotes AQP2 membrane accumulation, resulting in a marked reduction in urine output. We hypothesize that SCT stimulation alone activates an intracellular pathway leading to AQP2 gene transcription with no apparent effect on membrane trafficking. FLU shows a pleiotropic effect on plasma membrane accumulation of AQP2. The combination of the two molecules also increases solute conservation/reabsorption, thus providing the osmotic gradient for water reabsorption.

These results are highly relevant for the development of novel pharmacological approaches for the treatment of human X-NDI. In particular, a combination of molecules that can increase AQP2 transcription and plasma membrane targeting may improve the beneficial effects of the current therapy and further reduce the polyuria of NDI patients with a positive impact on their quality of life.

MATERIALS AND METHODS

Abs and reagents

Rabbit polyclonal affinity-isolated Abs against actin and SCTR (cat.# HPA007269), collagenase (cat.# C0130), and hyaluronidase (cat.# H3506) were from Sigma (www.sigmaaldrich.com). Goat anti-AQP3, goat anti-Na^+/K^+-ATPase, rabbit anti-Tamm-Horsfall, and mouse anti-AQP2 Abs were from Santa Cruz Biotechnology (www.scbt.com). Rabbit affinity-purified polyclonal Abs against human AQP2 were previously described.[10] dDAVP and 4-OH-TAX were purchased from Sigma, and rat SCT from Chiscientific (www.chiscientific.com). FLU sodium salt was purchased from Sequoia Research Products (www.seqchem.com).

RNA isolation, RT-PCR, and RT-quantitative PCR

Total RNA was extracted from adult mouse kidney and pancreas by the TRIzol extraction method (TRIzol reagent, Life Technologies, Invitrogen, Carlsbad, CA). The RNA was then used to amplify fragments of the complementary DNA of the AQPs using SuperScript VILO cDNA Synthesis Kit One-Step RT-PCR (Life Technologies). The primers (forward: 5′-ACCTGCTGAAGCTCAAGGC-3′, reverse: 5′-GTCATCTGCGGGGAAGAGTA-3′) were designed on the basis of the *mus musculus* SCTR nucleotide sequences available in the GenBank database (web site: http://www.ncbi.nlm.nih.gov/nuccore). The primers pair was chosen to hybridize with complementary DNA sequences derived from different exons (6 and 7), thereby excluding those amplimers arising from genomic DNA contamination. A positive control was performed by using primers specific for mouse β-actin complementary DNA. PCRs were performed with the following program:

(94 °C, 5 min) × 1 cycle;

(94 °C, 45 s; 59 °C, 30 s; 72 °C, 30 s) × 40 cycles.

The PCR products were separated on a 3% agarose gel and were visualized with ethidium bromide.

For quantification of AQP2 mRNA, total RNA was extracted using Trizol (Invitrogen). RNA was reverse transcribed and real-time PCR was performed in triplicate using the Applied Biosystems StepONE Real-time PCR system and TaqMan GenExpression Assays (Life Technologies, part no.:4331182) for mouse AQP2 (Life Technologies, Mm 00437575 Aqp2_m1). Mouse glyceraldehyde 3-phosphate dehydrogenase (Life Technologies, Mm 99999915_g1) was used as endogenous control. Each reaction was carried on as a singleplex reaction. The setup of reactions consisted of 1 µl of complementary DNA (20 ng), 1 µl of TaqMan Gene Expression Assay Mix, part no.: 4351370, 10 µl TaqMan Gene Expression Master Mix, catalog no.: 4369016, and 8 µl of Rnase-free water under the following PCR conditions: step 1, 95 °C for 10 min; step 2, 95 °C for 15 s; and step 3, 60 °C for 1 min; steps 2 and 3 were repeated 40 times.

The relative quantification of target gene expression was evaluated with data from the Step-ONE software (Foster City, CA), using the arithmetic formula $2^{-\Delta\Delta Ct}$, according to the comparative Ct method, which represents the amount of target, as normalized to the *glyceraldehyde 3-phosphate dehydrogenase* endogenous control (reference).

Tissue fractionation and immunoblotting

Whole-kidney or kidney CTX, OM, and IM were isolated from Wt C57BL/6 or $V2R^{fl/y}$*Esr1-Cre* mice and homogenized using an Heidolf tissue homogenizer (http://www.heidolph-instruments.com) at 1250 r.p.m. in 2 ml RIPA buffer (150 mmol/l NaCl, 10 mmol/l Tris, pH 7.2, 0.1% sodium dodecyl sulfate, 1% Triton X-100, 1% deoxycholate, 5 mmol/l EDTA) containing protease inhibitors (1 mmol/l phenylmethylsulfonyl fluoride, 10 µmol/l leupeptin, 1 µg/ml pepstatin, 10 mmol/l NaF, 1 mmol/l sodium orthovanadate, and 15 mmol/l tetrasodium pyrophosphate). Unbroken cells and nuclei were pelleted by centrifugation at 13,000×*g* for 30 min at 4 °C. An amount of 30 µg of each supernatant was separated by standard sodium dodecyl sulfate–polyacrylamide gel electrophoresis and analyzed by western blotting.

Protein samples, diluted in Laemmli's buffer with 50 mmol/l dithiothreitol, were heated for 10 min at 60 °C, resolved on 12% sodium dodecyl sulfate-polyacrylamide gels, and then electrophoretically transferred to polyvinylidene difluoride membranes (Millipore, Billerica, MA) for western blot analysis.

After blocking with 3% bovine serum albumin in tris buffer saline-tween 20, blots were incubated overnight at 4 °C with the indicated primary Abs. Membranes were washed and incubated with horseradish peroxidase–conjugated secondary Abs. Reactive proteins were revealed with an enhanced chemiluminescent detection system (SuperSignal West Pico Chemiluminescent Substrate, Pierce, Rockford, IL) and chemiluminescence was detected with Chemidoc XRS detection system equipped with Image Lab Software for image acquisition (www.bio-rad.com).

The quantification of protein bands was performed by determination of the relative optical density using ImageJ software (National Institutes of Health, Bethesda, MD).

Abs and their corresponding dilutions were: mouse anti-actin (1:500, Sigma Aldrich), mouse anti-SCTR (1:300, Sigma Aldrich), goat anti-AQP3 (1:500, Santa Cruz Biotechnology), and rabbit anti-AQP2 (1:1000, affinity-purified Ab[10]).

Immunofluorescence

Mouse kidneys were fixed overnight with 4% paraformaldehyde at 4 °C, cryopreserved in 30% sucrose for 24 h, and then embedded in optimal cutting temperature medium. Ultrathin sections (4 µm) placed on Superfrost/Plus Microscope Slides (Thermo Scientific, Braunschweig, Germany) were subjected to immunofluorescence analysis. Nonspecific binding sites were blocked with 1% bovine serum albumin in phosphate-buffered saline (PBS) (saturation buffer) for 30 min at room temperature. Sections were then incubated with the primary Abs for 2 h at room temperature (dilutions: AQP2 affinity purified 1:1000; monoclonal AQP2 1:250; SCTR 1:300; THP 1:500; Na^+/K^+-ATPase 1:1000) in saturation buffer. After washing in PBS, sections were incubated with the appropriate AlexaFluor-conjugated secondary Ab (www.lifetechnologies.com) for 1 h at room temperature. After washing in PBS, sections were incubated with TO-PRO-3 Iodide (642/661) (1:10,000 in PBS, Life Technologies) for 10 min and were mounted in PBS/glycerol (1:1) containing 1% *n*-propylgallate, pH 8.0. Confocal images were obtained with a confocal laser-scanning fluorescence microscope (Leica TSC-SP2, Mannheim, Germany).

In situ kidney tissue slices: preparation and treatment

The effect of SCT on AQP2 trafficking was studied in thin kidney slices prepared from C57BL/6 mice.

Briefly, adult male mice were anesthetized with an i.p. injection of tribromoethanol (250 mg/kg; Sigma Aldrich) and killed by cervical dislocation. Kidneys were rapidly excised and thin transversally sliced kidneys (250 µm) were cut using a McILWAIN Tissue Chopper (Ted Pella, http://www.tedpella.com).

All of the slices were incubated at 37 °C for 15 min in equilibrated Dulbecco's modified Eagle's medium-F12 medium only. After equilibration, the slices were distributed into a multiwell plate containing either Dulbecco's modified Eagle's medium-F12 or dDAVP (10^{-7} mol/l) or SCT (10^{-7} mol/l) in Dulbecco's modified Eagle's medium-F12. After 60 min of incubation at 37 °C, all of the slices were fixed by immersion in 4% paraformaldehyde in PBS at 4 °C overnight. The slices were then rinsed several times in PBS before use for immunostaining as described above. The immunofluorescence protocol was the same but slices were incubated with saturation buffer and primary Ab overnight at 4 °C.

Preparation of IMCD tubule suspensions

IMs were dissected out from kidneys of C57BL/6 WT mice (10-week-old males), minced, and enzymatically digested in Dulbecco's modified Eagle's medium-F12 high glucose containing 0.3% collagenase and 0.3% hyaluronidase at 37 °C for 90 min. The resulting suspension was centrifuged at 80 *g* for 30 s. IMCD-enriched pellets were collected after three washes with medium culture to remove residual proteases.

cAMP assays

cAMP assays were performed using mouse IMCD tubule suspensions, which were prepared as described above. For each individual experiment, IMCD suspensions were prepared and pooled from the kidneys of seven C57BL/6 WT and X-NDI mice (12-week-old males). Aliquots of IMCD tubule suspensions were preincubated with the cAMP phosphodiesterase inhibitor 3-isobutyl-1-methylxanthine for 10 min at 37 °C.

Subsequently, different concentrations of SCT (10^{-8} mol/l to 10^{-5} mol/l) or dDAVP (10^{-9} mol/l to 10^{-6} mol/l) were added, and reactions were carried out for 30 min at 37 °C. Total intracellular cAMP was determined via enzyme-linked immunosorbent assay according to the manufacturer's instructions (cAMP Biotrak; GE

Healthcare, Buckinghamshire, UK). cAMP data were analyzed using Prism software (version 4.0; GraphPad Software, La Jolla, CA).

Animal studies

All animal experiments carried out were approved by the Institutional Committee on Research Animal Care, in accordance with the Italian Institute of Health Guide for the Care and Use of Laboratory Animals.

Mice were maintained on a 12-h light/12-h dark cycle, with free access to water and food.

Wt C57BL/6 mice (Harlan Laboratories (Indianapolis, IN), males, 8-week old) were used to obtain kidney slices.

The generation of conditional V2R mutant mice ($V2R^{fl/fl}$and $V2R^{fl/y}$*Esr1-Cre* mice) has been described previously.[15] To disrupt the *V2R* gene in $V2R^{fl/y}$*Esr1-Cre* mice and to induce the X-NDI phenotype, a stock solution of 4OH-TMX (Sigma), prepared in preheated ethanol (50 mg/ml), was diluted in corn oil to 5 mg/ml. Adult $V2R^{fl/y}$*Esr1-Cre* mice (age 7–8 weeks old) were given a daily i.p. injection of 4-OH-TMX (0.1 ml of a 5 mg/ml suspension) over 6 days.

Treatment with drugs

Animals were treated with SCT and/or FLU 5 months after the last TMX injection. Rat SCT was administered subcutaneously (1 nmol/kg/day) to X-NDI mice via an Alzet (www.alzet.com) osmotic pump model 1002 implanted in a pocket between the scapulae under anesthesia. The skin incision was sutured. Pumps were loaded with a 100 µl solution of 10 µg/ml SCT in sterile PBS and kept in place for 14 days. Control animals received pumps loaded with PBS alone.

On the 14th day, half of the animals received a single i.p. injection of FLU (50 mg/kg). Mice were placed into metabolic cages (Tecniplast, www.tecniplast.it). Urine output and osmolality, along with water consumption, were monitored daily. Urine osmolalities were measured using a vapor pressure osmometer (model 5520; Wescor, www.wescor.com).

Mice were anesthetized with tribromoethanol (250 mg/kg; Sigma Aldrich) and killed by cervical dislocation.

Urinary and plasma creatinine were measured by high-performance liquid chromatography following a protocol similar to that described by Procino *et al.*[24]

Determination of glomerular filtration rate

GFR of conscious mice was measured by fluorescein isothiocyanate-labeled sinistrin clearance after a single retro-orbital injection and consecutive blood sampling from the tail vein.[42]

DISCLOSURE

All the authors declared no competing interests.

ACKNOWLEDGMENTS

This work has been funded by grants from Fondazione Telethon N° GGP12040 to MS, Agenzia Italiana del Farmaco (AIFA) MRAR08P011 to MS, from PRIN (Research Program of National Interest) projects to MS (2009J53ALK), and from Fondo per gli Investimenti della Ricerca di Base-Rete Nazionale di Proteomica (RBRN07BMCT_009). JW and JHL were supported by the Intramural Research Program of the National Institute of Diabetes and Digestive and Kidney Diseases (NIH, Bethesda, MD). We are grateful to Professor Hayo Castrop and Dr Katharina Mederle for sharing their expertise on GFR measurements in conscious mice and to G Devito for animal care.

SUPPLEMENTARY MATERIAL

Figure S1. Loss of urinary concentrating ability in V2R-KO mice.
Figure S2. Immunoblots assessing protein abundance of the collecting duct aquaporin water channels AQP2 and AQP3.
Supplementary material is linked to the online version of the paper at http://www.nature.com/ki

REFERENCES

1. Bichet DG. V2R mutations and nephrogenic diabetes insipidus. *Prog Mol Biol Transl Sci* 2009; **89**: 15–29.
2. Robben JH, Knoers NV, Deen PM. Cell biological aspects of the vasopressin type-2 receptor and aquaporin 2 water channel in nephrogenic diabetes insipidus. *Am J Physiol Renal Physiol* 2006; **291**: F257–F270.
3. Wesche D, Deen PM, Knoers NV. Congenital nephrogenic diabetes insipidus: the current state of affairs. *Pediatr Nephrol* 2012; **27**: 2183–2204.
4. Boone M, Deen PM. Physiology and pathophysiology of the vasopressin-regulated renal water reabsorption. *Pflugers Arch* 2008; **456**: 1005–1024.
5. Hasler U, Leroy V, Martin PY *et al.* Aquaporin-2 abundance in the renal collecting duct: new insights from cultured cell models. *Am J Physiol Renal Physiol* 2009; **297**: F10–F18.
6. Knepper MA, Inoue T. Regulation of aquaporin-2 water channel trafficking by vasopressin. *Curr Opin Cell Biol* 1997; **9**: 560–564.
7. Moeller HB, Fenton RA. Cell biology of vasopressin-regulated aquaporin-2 trafficking. *Pflugers Arch* 2012; **464**: 133–144.
8. Nedvetsky PI, Tamma G, Beulshausen S *et al.* Regulation of aquaporin-2 trafficking. *Handb Exp Pharmacol* 2009; 133–157.
9. Tamma G, Procino G, Svelto M *et al.* Cell culture models and animal models for studying the patho-physiological role of renal aquaporins. *Cell Mol Life Sci* 2012; **69**: 1931–1946.
10. Tamma G, Procino G, Strafino A *et al.* Hypotonicity induces aquaporin-2 internalization and cytosol-to-membrane translocation of ICln in renal cells. *Endocrinology* 2007; **148**: 1118–1130.
11. Bouley R, Hawthorn G, Russo LM *et al.* Aquaporin 2 (AQP2) and vasopressin type 2 receptor (V2R) endocytosis in kidney epithelial cells: AQP2 is located in 'endocytosis-resistant' membrane domains after vasopressin treatment. *Biol Cell* 2006; **98**: 215–232.
12. Yasui M, Zelenin SM, Celsi G *et al.* Adenylate cyclase-coupled vasopressin receptor activates AQP2 promoter via a dual effect on CRE and AP1 elements. *Am J Physiol* 1997; **272**: F443–F450.
13. Deen PM, van Aubel RA, van Lieburg AF *et al.* Urinary content of aquaporin 1 and 2 in nephrogenic diabetes insipidus. *J Am Soc Nephrol* 1996; **7**: 836–841.
14. Kanno K, Sasaki S, Hirata Y *et al.* Urinary excretion of aquaporin-2 in patients with diabetes insipidus. *N Engl J Med* 1995; **332**: 1540–1545.
15. Li JH, Chou CL, Li B *et al.* A selective EP4 PGE2 receptor agonist alleviates disease in a new mouse model of X-linked nephrogenic diabetes insipidus. *J Clin Invest* 2009; **119**: 3115–3126.
16. Promeneur D, Kwon TH, Frokiaer J *et al.* Vasopressin V(2)-receptor-dependent regulation of AQP2 expression in Brattleboro rats. *Am J Physiol Renal Physiol* 2000; **279**: F370–F382.
17. Knoers N, Monnens LA. Nephrogenic diabetes insipidus: clinical symptoms, pathogenesis, genetics and treatment. *Pediatr Nephrol* 1992; **6**: 476–482.
18. Knoers NV, Deen PM. Molecular and cellular defects in nephrogenic diabetes insipidus. *Pediatr Nephrol* 2001; **16**: 1146–1152.
19. Bouley R, Breton S, Sun T *et al.* Nitric oxide and atrial natriuretic factor stimulate cGMP-dependent membrane insertion of aquaporin 2 in renal epithelial cells. *J Clin Invest* 2000; **106**: 1115–1126.
20. Bouley R, Hasler U, Lu HA *et al.* Bypassing vasopressin receptor signaling pathways in nephrogenic diabetes insipidus. *Semin Nephrol* 2008; **28**: 266–278.
21. Bouley R, Lu HA, Nunes P *et al.* Calcitonin has a vasopressin-like effect on aquaporin-2 trafficking and urinary concentration. *J Am Soc Nephrol* 2011; **22**: 59–72.
22. Li W, Zhang Y, Bouley R *et al.* Simvastatin enhances aquaporin-2 surface expression and urinary concentration in vasopressin-deficient Brattleboro rats through modulation of Rho GTPase. *Am J Physiol Renal Physiol* 2011; **301**: F309–F318.
23. Olesen ET, Rutzler MR, Moeller HB *et al.* Vasopressin-independent targeting of aquaporin-2 by selective E-prostanoid receptor agonists alleviates nephrogenic diabetes insipidus. *Proc Natl Acad Sci USA* 2011; **108**: 12949–12954.

24. Procino G, Barbieri C, Carmosino M *et al.* Fluvastatin modulates renal water reabsorption in vivo through increased AQP2 availability at the apical plasma membrane of collecting duct cells. *Pflugers Arch* 2011; **462**: 753–766.
25. Russo LM, McKee M, Brown D. Methyl-beta-cyclodextrin induces vasopressin-independent apical accumulation of aquaporin-2 in the isolated, perfused rat kidney. *Am J Physiol Renal Physiol* 2006; **291**: F246–F253.
26. Los EL, Deen PM, Robben JH. Potential of nonpeptide (ant)agonists to rescue vasopressin V2 receptor mutants for the treatment of X-linked nephrogenic diabetes insipidus. *J Neuroendocrinol* 2010; **22**: 393–399.
27. Jean-Alphonse F, Perkovska S, Frantz MC *et al.* Biased agonist pharmacochaperones of the AVP V2 receptor may treat congenital nephrogenic diabetes insipidus. *J Am Soc Nephrol* 2009; **20**: 2190–2203.
28. Robben JH, Kortenoeven ML, Sze M *et al.* Intracellular activation of vasopressin V2 receptor mutants in nephrogenic diabetes insipidus by nonpeptide agonists. *Proc Natl Acad Sci USA* 2009; **106**: 12195–12200.
29. Chu JY, Yung WH, Chow BK. Secretin: a pleiotrophic hormone. *Ann N Y Acad Sci* 2006; **1070**: 27–50.
30. Trimble ER, Bruzzone R, Biden TJ *et al.* Secretin stimulates cyclic AMP and inositol trisphosphate production in rat pancreatic acinar tissue by two fully independent mechanisms. *Proc Natl Acad Sci USA* 1987; **84**: 3146–3150.
31. Chu JY, Chung SC, Lam AK *et al.* Phenotypes developed in secretin receptor-null mice indicated a role for secretin in regulating renal water reabsorption. *Mol Cell Biol* 2007; **27**: 2499–2511.
32. Charlton CG, Quirion R, Handelmann GE *et al.* Secretin receptors in the rat kidney: adenylate cyclase activation and renal effects. *Peptides* 1986; **7**: 865–871.
33. Velmurugan S, Brunton PJ, Leng G *et al.* Circulating secretin activates supraoptic nucleus oxytocin and vasopressin neurons via noradrenergic pathways in the rat. *Endocrinology* 2010; **151**: 2681–2688.
34. Glaser S, Lam IP, Franchitto A *et al.* Knockout of secretin receptor reduces large cholangiocyte hyperplasia in mice with extrahepatic cholestasis induced by bile duct ligation. *Hepatology* 2010; **52**: 204–214.
35. Wang X, Ye H, Ward CJ *et al.* Insignificant effect of secretin in rodent models of polycystic kidney and liver disease. *Am J Physiol Renal Physiol* 2012; **303**: F1089–F1098.
36. Holtmann MH, Roettger BF, Pinon DI *et al.* Role of receptor phosphorylation in desensitization and internalization of the secretin receptor. *J Biol Chem* 1996; **271**: 23566–23571.
37. Ozcelebi F, Holtmann MH, Rentsch RU *et al.* Agonist-stimulated phosphorylation of the carboxyl-terminal tail of the secretin receptor. *Mol Pharmacol* 1995; **48**: 818–824.
38. Shetzline MA, Premont RT, Walker JK *et al.* A role for receptor kinases in the regulation of class II G protein-coupled receptors. Phosphorylation and desensitization of the secretin receptor. *J Biol Chem* 1998; **273**: 6756–6762.
39. Kortenoeven ML, Trimpert C, van den Brand M *et al.* In mpkCCD cells, long-term regulation of aquaporin-2 by vasopressin occurs independent of protein kinase A and CREB but may involve Epac. *Am J Physiol Renal Physiol* 2012; **302**: F1395–F1401.
40. Ares GR, Caceres PS, Ortiz PA. Molecular regulation of NKCC2 in the thick ascending limb. *Am J Physiol Renal Physiol* 2011; **301**: F1143–F1159.
41. Hardcastle IR, Rowlands MG, Barber AM *et al.* Inhibition of protein prenylation by metabolites of limonene. *Biochem Pharmacol* 1999; **57**: 801–809.
42. Oppermann M, Mizel D, Kim SM *et al.* Renal function in mice with targeted disruption of the A isoform of the Na-K-2Cl co-transporter. *J Am Soc Nephrol* 2007; **18**: 440–448.